Diversity in the mechanisms of cosolute action on biomolecular processes

Shahar Sukenik, Liel Sapir, Regina Gilman-Politi and Daniel Harries*

Received 6th May 2012, Accepted 24th May 2012
DOI: 10.1039/c2fd20101a

Numerous cellular cosolutes significantly impact the way that proteins and other biomacromolecules act and interact. We have followed the thermodynamic effect of several cosolute classes, including polymers, cellular osmolytes, and inorganic salts, on the stability of biomolecular folding and complexation. By comparing changes in free energy, enthalpy, and entropy upon cosolutes addition for these processes, we identify several thermodynamically distinct mechanisms. Surprisingly, even while many cosolutes display similar scaling of the change in stabilizing free energy with their concentration, a breakdown of this free energy into enthalpic and entropic contributions distinguishes different families of cosolutes. We discuss how these "thermodynamic fingerprints" can direct towards possible underlying mechanisms that govern the cosolute effect.

1 Introduction

Salts and other cellular solutes profoundly affect the interactions between and within biomacromolecules.[1–11] Moreover, it is well appreciated that these effects are largely specific to the type of solute. As early as 1888, Hofmeister showed that some ions effectively precipitate or "salt out" many proteins from solution, while others help to solvate them.[12] This effect of salts is described by a common Hofmeister ranking of ions that has since been shown to extend to many other physical properties, including surface tension at the air–water interface, interactions and phase transitions in lipid membranes, and protein folding and complexation.[13–17] Over the past couple of decades, much effort has been devoted to gaining a better molecular-level understanding of these ion-specific effects at interfaces, as well as to developing quantitative predictive theories to account for the experimentally observed consequences of salt and other cosolute addition to macromolecular interactions.[18–26]

As our understanding of the cosolute-specific effects deepens, we seek further vindications and appropriate tests, while also attempting to extend our insight beyond the phenomenology and into the underlying molecular and thermodynamic mechanisms. In this effort, an important goal is to dissect the change in free energy upon cosolute addition into the associated contributions of enthalpy and entropy, forming a "thermodynamic fingerprint" for biomolecular processes in the presence of cosolutes. Through links to current theories that describe the forces driving macromolecular association or protein folding in the presence of cosolutes, this fingerprint should allow us to support or challenge different molecular mechanisms for different classes of cosolutes. A persistently lingering question remains: are there common unifying features in the mechanisms by which seemingly disparate

Institute of Chemistry and The Fritz Haber Research Center, The Hebrew University, Jerusalem, Israel. E-mail: daniel@fh.huji.ac.il

cosolutes, such as salts and neutral polyol osmolytes, exert their action on macromolecules?

In recent years there have been significant advances in linking the thermodynamics of cosolute action to specific mechanisms. It is now realized that while the changes in free energy may follow similar trends for different cosolutes, the underlying molecular driving forces can differ dramatically and, as a result, the breakdown into entropic and enthalpic contributions should vary. Macromolecular association that is driven by ion release, for example, shows an entropic gain upon binding due to the release of previously associated counterions from the macromolecular proximity.[28] For this mechanism, the addition of salt would, therefore, mainly impact the association entropy. Macromolecular crowding has also been shown to be entropically driven; the primary effect of molecularly large "crowders" is often due to their exclusion from a volume around proteins that drives burial of the macromolecular surfaces to allow subsequent favorable gains in free volume.[1] By contrast, we have previously shown that not all excluded cosolutes act in an entropy-driven mechanism. For example, small polyols, important "stabilizing osmolytes", were found to induce peptide folding primarily through enthalpic gains that are offset by a large unfavorable entropic contribution.[29] These cosolutes, used by cells to regulate cytoplasmic solution conditions with respect to their often deleterious environment, typically stabilize proteins in their folded state.[5,30] We have linked this favorable enthalpic contribution to folding due to cosolutes with the corresponding changes upon osmolyte addition to the hydrogen bond network of the waters surrounding the protein.[31] From these examples it already becomes clear that matching observed enthalpy–entropy thermodynamic fingerprints can help to support or rule out some of the possible underlying molecular mechanisms, and point to the potential applicability of others.

We have been using model biomolecules to help dissect the different contributing interactions that, in concert, modulate the response of proteins to the addition of cosolutes in aqueous solution. We start here by describing the effect of various salts on the association of β-cyclodextrin with adamantane, Fig. 1a. This guest–host complexation reaction involves the burial of uncharged, mostly nonpolar "hydrophobic" surfaces.[32,33] In the absence of direct electrostatic interactions between the cosolute and the interacting surfaces, we find that salt-specific stabilization of the complexed state follows the Hofmeister ranking of ions. The added complex

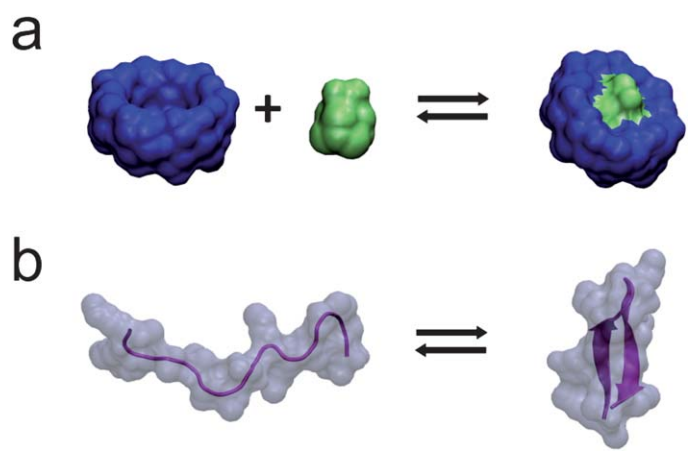

Fig. 1 Schematics of β-cyclodextrin association with adamantane carboxylate (**a**), and of the folding of a 16-amino acid long peptide (**b**). Representations demonstrate the decrease in solvent accessible surface area (SASA) in the complexation or folding process. Molecules rendered using VMD.[27]

stabilization can be well fit by integrated preferential interactions of salts with the surfaces of cyclodextrin and adamantane. This fit supports the Tanford–Bolen approach and that developed by Record and coworkers,[34,35,21,36] which ascribes additive transfer free energies to various surface groups in proportion to exposed surface area. The thermodynamic fingerprint of this complexation process reveals that complex stabilization by cosolute salt is dominated by a favorable entropic contribution with an added favorable enthalpic contribution at larger concentrations.

We next turn to follow the effect of cosolute addition on the folding of a model peptide into a β-hairpin, Fig. 1b. We have previously used naturally occurring "stabilizing osmolytes" to drive this folding process, and compared these osmolytes with the effect of molecularly larger PEG and dextran polymers, serving as "macromolecular crowders". Despite exhibiting a similar, size dependant stabilization effect on the peptide, the mechanisms observed for these two classes are disparate. While osmolytes stabilize folding through an enthalpic mechanism,[29] the larger PEGs and dextrans predominantly show entropic stabilization at low concentrations, which gradually takes on a larger enthalpic contribution as concentrations rise. This change with concentration seen in the thermodynamics may reflect a balance of entropically-driven excluded volume effects (or "depletion interactions") *versus* direct "chemical" interactions that can involve significant enthalpic contributions.

Finally, we address the effect of cosolute ions on the folding of the same peptide. As is often found for proteins, the charged peptide's stability responds to salts non-monotonically.[37,14,38] At low salt concentrations, we find peptide unfolding, while at higher concentrations there is regain of folding stability in an ion-specific manner that tracks the Hofmeister series. The changes at low salt concentrations can be assigned to electrostatic effects that can be reasonably described by Poisson–Boltzmann (PB) theory. The ion-specific stabilization effect seen at higher salt concentrations can be traced to the preferential interaction of salt with uncharged residues. The thermodynamic fingerprint for salts shows that, for the concentrations tested, they all act in an entropy-driven mechanism. Modeling the net effect of salts on folding as a sum of salt interactions with charged and uncharged surfaces suggests that the lower enthalpic contribution results from a cancelation of interaction of salts with the two types of surfaces.

By presenting this series of molecular models, we demonstrate how tracing the entropic and enthalpic contributions of cosolute action allows further insights into plausible underlying molecular mechanisms. Moreover, this strategy highlights remaining challenges in formulating quantitative theories to predict the cosolute effect on biomacromolecular processes.

2 Neutral interacting interfaces in the presence of cosolutes

To explore how different cosolutes influence biomacromolecular interactions, it is instructive to first consider interactions between neutral macromolecules, or study processes that involve burial or exposure of neutral, nonpolar, surfaces. Cosolute effects are simplified here since direct electrostatic interactions between the solute and cosolute become less significant. A useful example is the association of β-cyclodextrin (CD) and adamantane carboxylate and the impact on this complexation by various cosolutes, both neutral and charged.[39] Soluble CD is shaped as a truncated-cone with a hydrophobic cavity. Adamantane (AD) is highly insoluble in water, but when mixed with CD can associate to form an inclusion complex with increased solubility, Fig. 1a.

The CD/AD association is accompanied by a decrease in solvent accessible surface area (SASA) of about 400 $Å^2$, mainly associated with burial of nonpolar hydrophobic moieties. The preferential interaction of added cosolutes with CD and AD is generally different for the unassociated molecules and for the complex. Preferential exclusion of cosolute from the nonpolar macromolecular surfaces should lead to net stabilization of the complex, whereas preferential inclusion would result in

destabilization.[6,42,2,3] The extent of stabilization is quantified by the free energy of complexation, $\Delta\Delta G_{com}$, defined as $\Delta\Delta G_{com} = \Delta G_{com}(c) - \Delta G_{com}(0)$, where $\Delta G_{com}(c)$ and $\Delta G_{com}(0)$ are the free energies of complexation in cosolute solution of concentration c and in pure water, respectively. Isothermal titration calorimetry and vapor pressure osmometry experiments[43,39] have demonstrated that, for many cosolutes, $\Delta\Delta G_{com}$ is linear with respect to added cosolute concentration, Fig. 2a. Generally, salts stabilize the complex, whereas other solutes, such as betaine, destabilize it. The strength of the salt effect follows the Hofmeister ranking of anions, $SO_4^{2-} > F^- \approx Cl^- > Br^- > SCN^-$, seen as the differences in the slopes of the lines in Fig. 2a.

It is possible to predict $\Delta\Delta G_{com}$ by using the Tanford–Bolen and the Record approaches towards preferential solvation.[34,35,44] Such predictions are based on calculated changes in exposed surface areas for different chemical moieties, weighted by corresponding effective preferential interaction coefficients per unit area that are calibrated from transfer energies of model compounds.[21,44,36] To derive changes in exposed surface areas in CD/AD association, we performed all-atom molecular dynamics (MD) simulations of solutions of AD, CD, and the CD/AD complex in pure water using NAMD.[45] Water molecules were represented by the TIP3P potential and CD by the CHARMM-type CSFF model,[46] using MD simulation parameters as previously described.[47] The forcefield was appropriately extended to account for adamantane. The resulting molecular ensemble was used for SASA calculations of each species, where we have assumed that the conformational landscape of the complexed and unassociated molecules is unaltered by the presence of salt (while the ratio of complexed to uncomplexed molecules changes). Each configuration was assigned a SASA using the Richards set of atomic radii[35,44,48,49] and a 1.4 Å water probe radius, and these molecular surfaces were further decomposed into different classes (aliphatic, hydroxyl, or "other"). The contribution of each surface type to the change in free energy of transfer of the entire molecule (or complex) into each cosolute was then calculated using the available group transfer free energies (Table 1), while assuming group additivity.[21,44,36] Calculating the average transfer free energy for each separate molecule and for the complex allows calculation of $\Delta\Delta G_{com}$ due to the presence of salt, where $\Delta\Delta G_{com} = \Delta G_{CD+AD} - (\Delta G_{AD} + \Delta G_{CD})$, and terms on the right hand side represent the transfer free energy of the molecules from water into a solution containing cosolute at a specific concentration.

Assuming $\Delta\Delta G_{com}$ to be linear with cosolute osmolality (as is often found for weakly interacting or excluded cosolutes), we have predicted m-values, where the

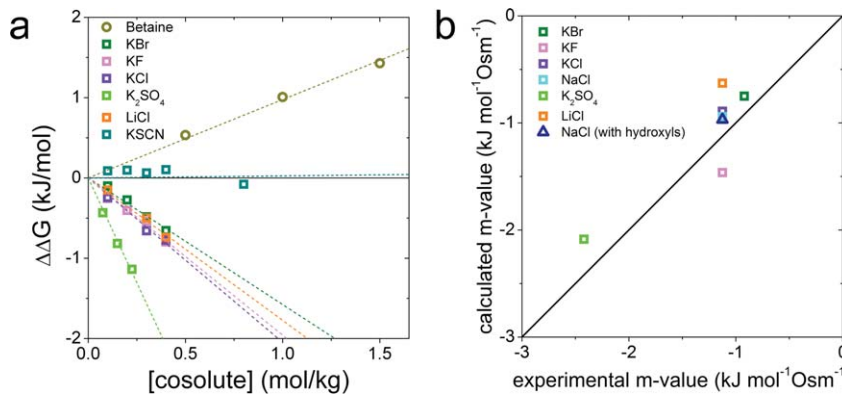

Fig. 2 (**a**) Changes in the free energy of β-cyclodextrin association with adamantane *versus* cosolute concentration. Lines are linear fits of the data. (**b**) Calculated *versus* experimentally derived *m*-values. Data represented by the triangle is based on an alternate set of group transfer free energies that in addition ascribes a value for hydroxyl groups (Table 1) based on measurements of alcohol model compounds.[40,41]

Table 1 Group transfer free energies for various cosolutes used in this study

	Group transfer free energies, J mol^{-1} m^{-1} $Å^{-2}$				
Cosolute	Aliphatic	Aromatic	Amide	Hydroxyl	Carboxyl
KBr[a]	4.2 ± 0.2	3.0 ± 0.5	−10 ± 1		
KF[a]	8.4 ± 0.2	5.9 ± 0.2	−11.4 ± 0.7		
KCl[a]	5.0 ± 0.2	4.2 ± 0.2	−10.4 ± 0.5		
NaCl[a]	5.5 ± 0.2	5.0 ± 0.2	−10.4 ± 0.5		
NaCl[b]	6.3 ± 0.5			−5 ± 2	
K_2SO_4[a]	13.9 ± 0.2	13.1 ± 0.5	−17 ± 1		
LiCl[c]	4.0 ± 0.5	4.0 ± 0.5	−9 ± 1		
GuHCl[a]	0.7 ± 0.2	−2.0 ± 0.5	−9 ± 1		
NH_4Cl[a]	2.0 ± 0.7		−3 ± 2		
Betaine[d]	0.87 ± 0.40	−5 ± 1	6 ± 1 (O) −4.2 ± 0.7 (N)	0.2 ± 0.3	6.9 ± 0.5

[a] Data by Pegram *et al.*44 The values for K_2SO_4 were derived from the available data on NaCl, KCl and Na_2SO_4, assuming ion-additivity. [b] Values were determined by analyzing salting out constants for various alcohols in NaCl41,40 according to the procedure described in ref. 21. [c] Derived from ref. 21 and 44 by globally fitting the solubility data. [d] Data by Capp *et al.*36

m-value is defined here by $\Delta\Delta G_{com} = mc_{Osm}$, for the complexation reaction, and c_{Osm} is the cosolute concentration on the osmolal scale.[50–53] These values are compared with experiment in Fig. 2b. The *m*-values show quantitatively excellent fits for KCl, KBr, and K_2SO_4, and fits for the other salts are close to the experimental and calculation errors. By contrast, the effect predicted for betaine is stabilizing ($m = -0.36$ kJ mol^{-1} Osm^{-1}), while experiments show a destabilizing effect on the complex ($m = 0.98$ kJ mol^{-1} Osm^{-1}) that suggests preferential inclusion of betaine in the solute vicinity. This discrepancy is probably due to cooperative effects of the segments of the convex inner interface of CD on the favorable association with betaine, a relatively large molecule with respect to simple inorganic ions. This may suggest that the group transfer free energies per surface area are non-additive in special cases where interacting surfaces are structured very differently from expanded, well-exposed, or flat interfaces. For such convex or corrugated interfaces (relative to the cosolute's size) the transfer free energy may scale nonlinearly with surface area.

We conclude that the free energy change upon addition of cosolute as determined by the Record approach allows fair estimates of the experimental *m*-values. In addition, decomposition of SASA to the different moieties to which transfer free energies are assigned works best when the different SASA elements are decoupled. However, when such coupling does exist, surface convexity and cosolute size become important, and could result in non-additive free energy contributions. In addition, we expect some discrepancies may result when not all group types are accounted for in the overall molecular SASA. Indeed, we find that by including the hydroxyl group transfer free energy into NaCl solutions, the fit of predicted and experimental *m*-value was improved, though only very slightly (compare the blue square and triangle in Fig. 2b). We note, finally, that taking group transfer free energy to be linear with either osmolal or molal concentration result in almost indistinguishable predictions for the concentration range used here.

3 Charged peptide in the presence of neutral cosolute

Protein folding poses additional challenges for analysis. Beyond non-polar hydrophobic residues, the macromolecular protein–water interface itself may carry

charges, so that subtle changes to the solvating environment can strongly impact the stability of the folded and unfolded protein conformational ensembles. For simplicity, we first describe the effect of non-electrolytes on peptide folding. The model system we used in these studies is a 16 amino-acid peptide previously described[54] that carries a net-total of +3 elementary charges at neutral pH. The peptide was determined in circular dichroism and NMR experiments to fit a two-state folding process from the unfolded to folded, β-hairpin states, Fig. 1b. We have followed the effect of two electrostatically neutral cosolute classes on the stability of this peptide. The first includes stabilizing osmolytes: sugars, such as the dissacharide trehalose, as well as polyols, including sorbitol, glycerol, erythriol, manitol, and xylitol. The second cosolute group consists of "macromolecular crowding" polymers, including various molecular weights of polyethylene glycol (PEG 100, 400, and 4000) and dextran (20 k and 40 k).

Molecular crowding theory has been proposed to rationalize the observed discrepancies between macromolecular interactions in the crowded milieu of the cell and *in vitro* experiments performed in dilute aqueous solutions. Briefly, by taking up volume in solution, non-interacting or "excluded" cosolutes promote any process that results in freeing up of space excluded by the macromolecules, or in liberating translational and conformational degrees-of-freedom for cosolutes. Such crowding has been shown to drive protein folding,[55,56] complexation,[57] and aggregation.[56,58] The magnitude of this stabilization scales with the molecular size of the cosolute. Indeed, the changes in free energy have been accurately predicted by using scaled particle theory for protein association in the presence of various macromolecular crowders including dextran.[58]

Using circular dichroism spectroscopy to monitor the change in free energy of peptide folding with increasing cosolute concentrations, we find that all cosolutes tested here stabilize the folded state. In addition, the change in free energy for the folding process, $\Delta\Delta G$, is linear with cosolute concentration, Fig. 3. This linearity is characteristic of stabilization through non-specific interactions, and similar trends have been shown for other folding and interacting proteins upon addition of these and other cosolutes.[59–61,44] The change in free energy is proportional to the size of the perturbing cosolute, as might also be expected for macromolecular crowders. Interestingly, however, our recent experiments[29] showed that for polyol osmolytes, the stabilizing mechanism is dominated by a favorable enthalpy, which cannot be accounted for by the simple molecular crowding model alone. As we further discuss

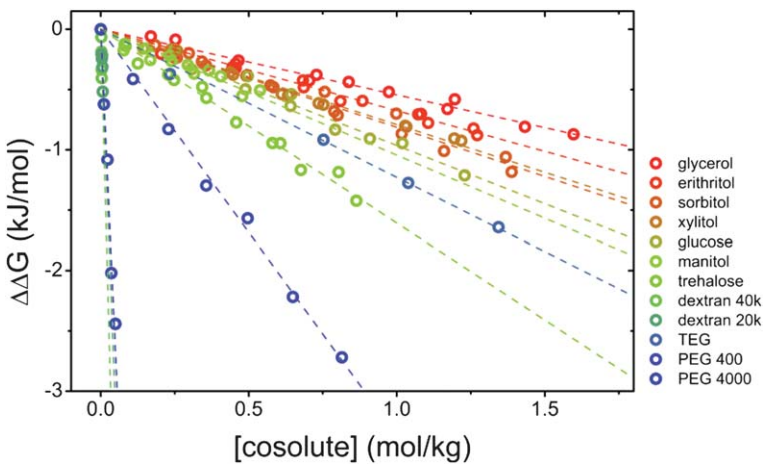

Fig. 3 Change in free energy of peptide folding with cosolute concentration. Dashed lines are linear fits of the data.

in section 5, these findings may indicate a fundamental mechanistic difference between the effects of macromolecular crowders and stabilizing osmolytes.

4 Charged peptide in the presence of salt

Because both electrolytes and protein are charged, their interactions can show the most complex cosolute effects, so that both electrostatic and "chemical" or ion-specific preferential interactions must be considered. We used circular dichroism spectroscopy to follow folding of the model peptide presented in section 3 in various salts at several concentrations. These data allow us to derive the change in free energy of folding, $\Delta\Delta G$, in the presence of the cosolute salts, Fig. 4. At low concentrations (less than ~0.25 M) all salts destabilize the native conformation of the peptide. As salt concentration increases, however, a stabilizing effect becomes prominent for most salts at concentrations higher than ~0.5 M, leading to a maximum in $\Delta\Delta G$. This type of non-monotonic behavior is often encountered for proteins.[37,38] For the more strongly destabilizing salts, GuHCl and to a lesser extent NH_4Cl, $\Delta\Delta G$ continues to rise with salt concentration, albeit with a reduced slope.

The Hofmeister ranking of ions dictates that certain cations and anions more strongly confer stability to proteins than others.[14,12] The classical Hofmeister ranking for the ions we have used, listed from the most stabilizing to the most destabilizing, is: for anions $SO_4^{2-} > Cl^-$, and for cations $Na^+ > K^+ > Li^+ > NH_4^+ > Gu^+$. Notably, our results follow this ranking, showing that the peptide stabilizing effects are strongest (when comparing anions) for Na_2SO_4, followed by NaCl and (comparing cations) are largest for NaCl, followed by KCl, LiCl, NH_4Cl, and finally GuHCl, which is most destabilizing towards the peptide.

Pegram and Record[44] were able to successfully account for the unfolding process of a different protein, the *lac*-protein DNA binding domain, by fitting the energetic contributions of the unfolding process to a functional form that accounts for electrostatic and ion-specific terms due to salt addition. The latter terms were predicted quite accurately by summing contributions to polar and non-polar peptide groups, derived by calculating the changes in SASA in the folded and unfolded states with calibrated group transfer free energies, as described in section 2. Using a similar approach, we have tried to fit the data in Fig. 4 with a sum of electrostatic and ion-specific contributions. In addition, we directly calculated the electrostatic free energy by numerically solving the nonlinear Poisson–Boltzmann (PB) equation. These electrostatic contributions were summed with the preferential interaction estimates, determined as described in section 2.

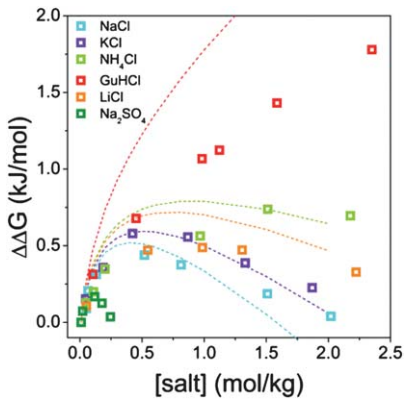

Fig. 4 Free energy of peptide folding as a function of salt concentration. Calculated values derived from the addition of PB and preferential interaction energies are shown as dashed lines.

To account for the electrostatic contribution to the folding free energy, folded and unfolded conformations were chosen from a peptide ensemble derived from all-atom MD simulations in explicit water.[31] The unfolded ensemble was obtained by sampling over 800 conformations that fulfilled a criteria based on SASA (>2300 Å^2). All conformations were assigned charges according to the CHARMM potential to the net-charged moieties only. This was done to avoid double-counting of ions around net-neutral surfaces that are separately accounted for in the preferential interaction energies; this procedure significantly improved the subsequent fits with experiments. The PB equation was solved numerically using APBS[62] for each conformation using the same grid dimensions, at different uni-univalent salt concentrations in the concentration range 0.01–2.0 M, The change in PB free energy for folding ($\Delta\Delta G_{PB}$) is the difference in the charging free energy G_{PB} values for the unfolded and the folded conformations at a specific salt concentration.

The predictions of $\Delta\Delta G$, evaluated as the sum of calculated transfer free energy for uncharged surfaces and PB electrostatics for charged groups, are shown as dashed lines in Fig. 4. While the trends and ordering of all salts from experiments are faithfully reproduced, we do not find a full quantitative match. This may be a result of ion-specific effects that are absent from the PB calculations, yet could become important, particularly at higher salt content. We and others have previously shown that modified PB equations can be used to properly account for this added salt-contribution.[63,64] However, these formulations require additional knowledge of the non-electrostatic preferential interaction of ions with the *charged* moieties, which is at present lacking for peptides.[65,66]

In an attempt to more faithfully reproduce the experimental values, we tested four different ensembles for both folded and unfolded conformations. These included trajectories derived from replica-exchange MD, implicit solvation models and additional MD simulations (for descriptions of these simulation methodologies see for example ref. 67 and 68). Because all ensembles were derived under pure water conditions, we also tested reassigning probabilities to conformations in the ensemble according to predicted shifts in free energy upon salt addition, which also contributed to changes in the average differences in free energies. While the energies for preferential interactions of ions with the non-charged peptide surface were relatively insensitive to the choice of ensemble, the energies derived from the electrostatic PB calculations showed large variations with the choice of ensemble. In contrast with the folded ensemble that had relatively low variability (standard deviation) for all the ensembles we tested, the energies derived for the unfolded conformations were more variable. Some forcefields tended to yield more extended, linear conformations, while others show more compact forms. The sensitivity we find underscores a significant challenge for protein stability predictions, because proper sampling is clearly essential for quantitative estimates. Importantly, our prediction estimates of $\Delta\Delta G$ can only be considered to be semi-quantitative. Fig. 4 shows the ensemble that best fit the experimental results for NaCl (the salt for which PB is usually most accurate). The unfolded ensemble is composed of roughly 800 conformations, taken from a 50 ns MD ensemble in explicit TIP3P waters. In addition, in line with the approach that takes folded proteins using a single or few experimentally determined states, we represent the folded state by a single conformation. While the theory seems to properly reproduce the trends in the ranking of ions and their effect on peptide stability, it is hard to give quantitatively exact predictions. The most sensitive element of modeling remains the electrostatic contributions related to ion–charged residue interactions.

5 Thermodynamic fingerprints characterizing mechanistic differences in cosolute effect

The breakdown of folding free energy into its enthalpic and entropic contributions affords new insight into the mechanisms by which different cosolute families exert

their stabilizing or destabilizing actions. We have measured the peptide folding free energy in the presence of various cosolutes, at different concentrations and at different temperatures, to determine the respective changes in enthalpy and entropy using a van 't Hoff analysis. These values are then subtracted from the enthalpy–entropy values for the peptide folding in buffered aqueous solution to obtain $\Delta\Delta H$ and $T\Delta\Delta S$ values, where $T = 298.15$ K (for additional information see ref. 29). A similar decomposition was performed for CD/AD association using isothermal titration calorimetry.[39] We find a clear separation of different cosolute families in the resulting entropy–enthalpy plots, whereby the distinct groups tend to occupy different regimes of the plot, Fig. 5.

The diagonal line in Fig. 5, representing full enthalpic–entropic compensation, separates stabilizing cosolutes that lie above it (blue area highlighted in the inset of Fig. 5a) from those causing destabilization lying beneath it (pink area). The stabilizing region can be further divided into two specific regions corresponding to different underlying thermodynamic effects. Region I includes solutes showing an enthalpically driven stabilization, while cosolutes that fall within region II induce increased stability that is primarily entropically driven. Similarly, regions III and IV indicate an enthalpic and entropic destabilizing effect, respectively. For the CD/AD complexation process (discussed in section 2), all salts tested stabilize the complex *via* an entropically dominated process (region II) at low concentrations, while at higher concentrations the effect becomes more enthalpically driven (region I), Fig. 5a.

For the peptide folding process, the stabilizing cosolutes tested include polyol osmolytes as well as the larger, polymeric crowders PEG and dextran, Fig. 5b. Polymers span much of the upper left area of the plot, moving from an entropically dominated mechanism at lower concentrations (region II) to a larger enthalpic contribution to their stabilizing effect (region I) at higher concentrations. All polyols, by contrast, fall close to a single line, which represents an enthalpic stabilizing effect (region I). This effect is generally weaker than for the polymers at a given concentration, seen as a shorter distance of data points from the diagonal. This difference in thermodynamic fingerprint is surprising, as there is no hint to this apparent difference in mechanism in the data shown in Fig. 3, where we find the same trend and scaling of $\Delta\Delta G$ with cosolute molecular size for both cosolute types.

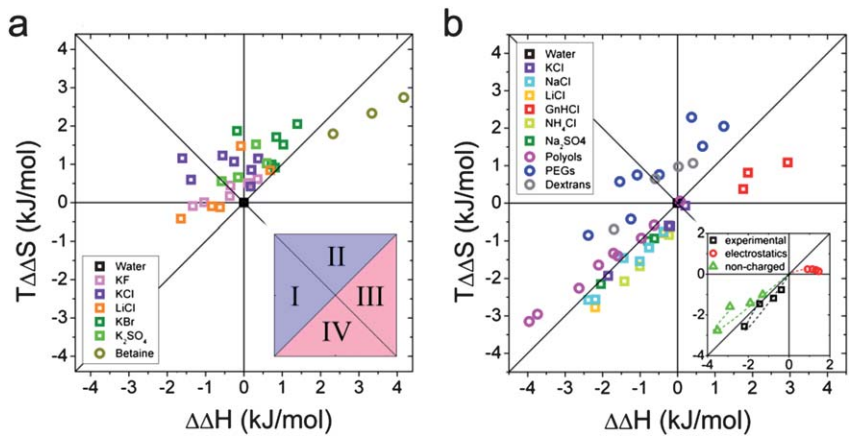

Fig. 5 Entropy *versus* enthalpy plots for changes in macromolecular processes upon cosolute addition. (**a**) CD/AD complexation. Inset shows the different corresponding regimes on the plot, and the blue and red colors signify stabilizing and destabilizing regions, respectively; see text for details. (**b**) Folding of a peptide. Inset shows the model enthalpic and entropic contributions to charged (PB) and non-charged terms of electrolytes on peptide folding.

The disparities seen in the thermodynamic fingerprint bespeak mechanistic differences in cosolute stabilizing effect for the polyol osmolytes *versus* the polymeric crowders. We have previously traced the enthalpically driven stabilization induced by osmolytes to the reordering of the hydrogen bond network in aqueous solution in the presence of the polyols.[31,69] Polymeric crowders, on the other hand, have long been shown to act in an entropically driven fashion through steric, excluded volume interactions,[59] as also described in section 1. Interestingly, recent evidence shows that at high concentration the mechanism of action may change for these crowder molecules. Record and coworkers have found that while PEG induces a stabilizing effect on DNA duplexation at low cosolute concentration, as predicted by molecular crowding theory, high concentrations show a destabilizing trend that has been attributed to the formation of a "mesh" of polymer molecules which comes into direct interaction with the DNA surface.[70] We propose that a similar balance of forces may explain the shift we find from entropically to enthalpically driven peptide folding at intermediate polymer concentrations.

The denaturing cosolute regime occupies the area below the full-compensation diagonal (regions III and IV). Here we find salts that tend to have an overall destabilizing effect on the model peptide (discussed in section 4). Over the entire concentration range tested, all salts, except GuHCl, promote entropically driven destabilization (region IV). GuHCl represents a special electrolytic cosolute since it bears a charge but also shows strong preferential inclusion to peptides and proteins that are not purely electrostatic.[71] We find that GuHCl shows a strong enthalpic denaturing effect, probably due to appreciable binding to the peptide, and accordingly its thermodynamic fingerprint lies in region III.

The model calculations we have performed (detailed in section 4) dissect the effect of salts into contributions from electrostatics and preferential (or ion-specific) interactions, $\Delta\Delta G_{exp} = \Delta\Delta G_{PB} + \Delta\Delta G_{m}$. It is, therefore, possible to further decompose these variations in free energy into enthalpic and entropic contributions, by requiring that the contributions too must sum up to the experimental total changes in entropies and enthalpies. Thus, we have derived the enthalpic and entropic contributions to the PB free energy. We then derived the corresponding contributions to $\Delta\Delta G_{m}$, the transfer free energy of the uncharged surfaces for NaCl. Because the sum of PB and preferential interaction contributions (Fig. 4, dashed lines) does not completely overlap the experimental data, the values obtained from this breakdown should only be considered as semi-quantitative. Nonetheless, the trends that appear using this analysis are rather insensitive to the quality of the fit seen in Fig. 4.

We find that the free energy contribution to the interaction of ions with the charged surfaces, $\Delta\Delta G_{PB}$, is enthalpically destabilizing (region III), while the interaction with the non-charged surface $\Delta\Delta G_{m}$ falls in the same region as the polyol osmolytes, and is enthalpically stabilizing (region I), Fig. 5 inset. While the interaction of salts with both the charged and non-charged surfaces of the protein is enthalpically driven, the two contributions cancel each other to a large extent, and the sum of these interactions creates an overall destabilizing, yet entropically dominated change in folding free energy, as seen in Fig. 5b.

Comparing Fig. 5b with its inset suggests a possible common mechanism for the non-electrostatic salt–peptide interaction and for the polyol–peptide interactions. For both, the thermodynamic fingerprint is stabilizing and localized in region I. This resonates with the "kosmotropic" nature of some salts – a term used to describe the order-inducing tendencies of salts in water.[14,13] Indeed, our simulations of peptide folding have pointed to the strengthening of water's hydrogen-bonds in the vicinity of polyol cosolutes as the source for peptide stabilization.[31] Possibly, both polyol osmolytes and salts that interact with non-polar surfaces act through similar cosolute-induced "water order" or water structuring.

Interestingly, while the salt induced CD/AD complex stabilization is entropically driven, Fig. 5a, the calculated non-PB contribution of the same salts to the peptide folding process is enthalpically driven, Fig. 5b (inset). This difference could be

reconciled in at least two possible ways. First, the processes of peptide folding and CD/AD complexation involve changes in exposed surface area carrying different (chemical) propensities that could lead to different mechanisms. Alternatively, simple electrostatic PB calculations cannot account for ion-specific effects, so that more accurate approximations are possibly required. These could change the estimated interaction free energy with charged residues in the presence of different salts.

6 Concluding remarks

Control of cosolute content and concentrations is an integral means of cellular regulation and adaptation. While typically lacking strong, specific interactions, these cosolutes are nonetheless able to induce a measurable effect on the stability of many biological molecules and impact the way they interact. Here we have compared the action of several families of cosolutes: sugars and polyols, polymers, and salts, by measuring their effects on distinct macromolecular processes such as association and folding. Following the unique enthalpic–entropic fingerprint of each cosolute, we have found that certain cosolutes act through thermodynamically similar mechanisms that correlate with their chemical and physical characteristics. This fingerprinting allows to naturally separate cosolutes into families according to their common action, and sheds new light on the possible underlying mechanisms of cosolute effect. We suggest that similar analysis could be helpful not only in resolving the behavior of additional cosolutes, but also in formulating and testing predictive theories of their impact on macromolecular processes. Beyond thermodynamic changes in stability, we have recently shown that polyols and PEG crowders have disparate effects also on the kinetics of peptide amyloid aggregation.[56,72] Different salts, too, can differently influence kinetic steps (such as association *versus* dissociation) in molecular complexation.[43,73] We propose that there could be a possible mechanistic link between these kinetic changes and the corresponding thermodynamic mechanism we find for the different cosolute families. These types of links may eventually reshape our understanding of the way solvating environments are actively involved in numerous biochemical processes.

Acknowledgements

We thank D. Avnir for use of the circular dichroism spectrometer. DH acknowledges support from the Israel Science Foundation (ISF grants 1011/07, 1012/07). The Fritz Haber Center is supported by the Minerva Foundation, Munich, Germany.

References

1 R. J. Ellis and A. P. Minton, *Nature*, 2003, **425**, 27–28.
2 S. N. Timasheff, *Proc. Natl. Acad. Sci. U. S. A.*, 2002, **99**, 9721–9726.
3 V. A. Parsegian, *Int. Rev. Cytol.*, 2002, **215**, 1–31.
4 P. H. Yancey, M. E. Clark, S. C. Hand, R. D. Bowlus and G. N. Somero, *Science*, 1982, **217**, 1214–1222.
5 G. N. Somero, C. B. Osmond, and C. L. Bolis, *Water and life: comparative analysis of water relationships at the organismic, cellular, and molecular levels*, Springer-Verlag, 1992.
6 D. Harries and J. Rösgen, *Methods Cell Biol.*, 2008, **84**, 679–735.
7 Z. Ignatova and L. M. Gierasch, *Proc. Natl. Acad. Sci. U. S. A.*, 2006, **103**, 13357–13361.
8 B. W. Berger, C. M. Gendron, A. M. Lenhoff and E. W. Kaler, *Protein Sci.*, 2006, **15**, 2682–2696.
9 A. Nayak, C.-C. Lee, G. J. McRae and G. Belfort, *Biotechnol. Prog.*, 2009, **25**, 1508–1514.
10 R. Sousa, *Acta Crystallogr., Sect. D: Biol. Crystallogr.*, 1995, **51**, 271–277.
11 A. Kumar, P. Attri and P. Venkatesu, *Thermochim. Acta*, 2012, **536**, 55–62.
12 F. Hofmeister, *Arch. Pharmacol.*, 1888, **24**, 247–260.
13 K. D. Collins and M. W. Washabaugh, *Q. Rev. Biophys.*, 1985, **18**, 323–422.
14 W. Kunz, *Specific Ion Effects*, 1st edn, 2009.

15 H. I. Petrache, S. Tristram-Nagle, D. Harries, N. Kucerka, J. F. Nagle and V. A. Parsegian, *J. Lipid Res.*, 2006, **47**, 302–309.
16 H. I. Petrache, *Proc. Natl. Acad. Sci. U. S. A.*, 2006, **103**, 7982–7987.
17 L. M. Pegram and M. T. Record, *J. Phys. Chem. B*, 2007, **111**, 5411–5417.
18 R. L. Baldwin, *Biophys. J.*, 1996, **71**, 2056–2063.
19 P. Jungwirth and D. J. Tobias, *Chem. Rev.*, 2005, **106**, 1259–1281.
20 W. Kunz, P. Lo Nostro and B. W. Ninham, *Curr. Opin. Colloid Interface Sci.*, 2004, **9**, 1–18.
21 L. M. Pegram and M. T. Record, *J. Phys. Chem. B*, 2008, **112**, 9428–9436.
22 J. Rösgen, B. M. Pettitt, D. W. Bolen and J. Rosgen, *Biophys. J.*, 2005, **89**, 2988–2997.
23 D. Shukla, C. P. Schneider and B. L. Trout, *Adv. Drug Delivery Rev.*, 2011, **63**, 1074–1085.
24 M. H. Priya, H. S. Ashbaugh and M. E. Paulaitis, *J. Phys. Chem. B*, 2011, **115**, 13633–13642.
25 R. Chitra and P. E. Smith, *J. Phys. Chem. B*, 2001, **105**, 11513–11522.
26 T. Ghosh, A. Kalra and S. Garde, *J. Phys. Chem. B*, 2005, **109**, 642–651.
27 W. Humphrey, A. Dalke and K. Schulten, *J. Mol. Graphics*, 1996, **14**, 33–38.
28 M. T. Record, C. F. Anderson and T. M. Lohman, *Q. Rev. Biophys.*, 1978, **11**, 103–178.
29 R. Politi and D. Harries, *Chem. Commun.*, 2010, **46**, 6449–6451.
30 P. H. Yancey, *Integr. Comp. Biol.*, 2001, **41**, 699–709.
31 R. Gilman-Politi and D. Harries, *J. Chem. Theory Comput.*, 2011, 3816–3828.
32 B. C. Gibb, *Isr. J. Chem.*, 2011, **51**, 798–806.
33 M. V. Rekharsky and Y. Inoue, *Chem. Rev.*, 1998, **98**, 1875–1918.
34 K. C. K. C. Aune and C. Tanford, *Biochemistry*, 1969, **8**, 4586–4590.
35 M. Auton and D. W. Bolen, *Proc. Natl. Acad. Sci. U. S. A.*, 2005, **102**, 15065–15068.
36 M. W. Capp, L. M. Pegram, R. M. Saecker, M. Kratz, D. Riccardi, T. Wendorff, J. G. Cannon and M. T. Record, *Biochemistry*, 2009, **48**, 10372–10379.
37 R. Komsa-Penkova, R. Koynova, G. Kostov and B. G. Tenchov, *Biochim. Biophys. Acta, Protein Struct. Mol. Enzymol.*, 1996, **1297**, 171–181.
38 W. Kunz, *Pure Appl. Chem.*, 2006, **78**, 1611–1617.
39 D. Harries, D. C. Rau and V. A. Parsegian, *J. Am. Chem. Soc.*, 2005, 2184–2190.
40 Z. Sir, L. Strnadova and V. Rod, *Collect. Czech. Chem. Commun.*, 1980, **45**, 679.
41 G. Perron, D. Joly, J. E. Desnoyers, L. Avédikian and J.-P. Morel, *Can. J. Chem.*, 1978, **56**, 552–559.
42 J. Gibbs, in *The Scientific Papers of J. Willard Gibbs, Vol.1*, ed. H. Bumstead and R. van Name, Ox Bow, Woodbridge, CT, 1993.
43 P. A. Gurnev, D. Harries, V. A. Parsegian and S. M. Bezrukov, *ChemPhysChem*, 2009, **10**, 1445–1449.
44 L. M. Pegram, T. Wendorff, R. Erdmann, I. Shkel, D. Bellissimo, D. J. Felitsky and M. T. Record, *Proc. Natl. Acad. Sci. U. S. A.*, 2010, **107**, 7716–7721.
45 J. C. Phillips, R. Braun, W. Wang, J. Gumbart, E. Tajkhorshid, E. Villa, C. Chipot, R. D. Skeel, L. Kalé and K. Schulten, *J. Comput. Chem.*, 2005, **26**, 1781–1802.
46 M. Kuttel, J. W. Brady and K. J. Naidoo, *J. Comput. Chem.*, 2002, **23**, 1236–1243.
47 L. Sapir and D. Harries, *J. Phys. Chem. B*, 2011, **115**, 624–634.
48 G. D. Rose, A. R. Geselowitz, G. J. Lesser, R. H. Lee and M. H. Zehfus, *Science*, 1985, **229**, 834–838.
49 B. Lee and F. M. Richards, *J. Mol. Biol.*, 1971, **55**, 379–IN4.
50 R. A. Robinson and R. H. Stokes, *Electrolyte solutions*, Dover Publications, 2002.
51 B. Wishaw and R. Stokes, *Trans. Faraday Soc.*, 1953, **49**, 27–31.
52 D. J. Davis, C. Burlak and N. P. Money, *Mycol. Res.*, 2000, **104**, 800–804.
53 E. Courtenay, M. Capp, R. Saecker and M. Record Jr., *Proteins: Struct., Funct., Genet.*, 2000, **4**, 72–85.
54 A. J. Maynard, G. J. Sharman and M. S. Searle, *J. Am. Chem. Soc.*, 1998, **120**, 1996–2007.
55 M. S. Cheung, D. Klimov and D. Thirumalai, *Proc. Natl. Acad. Sci. U. S. A.*, 2005, **102**, 4753–4758.
56 S. Sukenik, R. Politi, L. Ziserman, D. Danino, A. Friedler and D. Harries, *PLoS One*, 2011, **6**, e15608.
57 N. Kozer and G. Schreiber, *J. Mol. Biol.*, 2004, **336**, 763–774.
58 D. M. Hatters, A. P. Minton and G. J. Howlett, *J. Biol. Chem.*, 2002, **277**, 7824–7830.
59 D. Hall and A. P. Minton, *Biochim. Biophys. Acta, Proteins Proteomics*, 2003, **1649**, 127–139.
60 M. Auton and D. W. Bolen, *Biochemistry*, 2004, **43**, 1329–1342.
61 J. C. Lee and S. N. Timasheff, *Biochemistry*, 1974, **13**, 257–265.
62 N. A. Baker, D. Sept, S. Joseph, M. J. Holst and J. a. McCammon, *Proc. Natl. Acad. Sci. U. S. A.*, 2001, **98**, 10037–10041.
63 D. Ben-Yaakov, D. Andelman, D. Harries and R. Podgornik, *J. Phys.: Condens. Matter*, 2009, **21**, 424106.

64 D. Ben-Yaakov, D. Andelman, R. Podgornik and D. Harries, *Curr. Opin. Colloid Interface Sci.*, 2011, **16**, 542–550.
65 A. P. dos Santos and Y. Levin, *Phys. Rev. Lett.*, 2011, **106**, 167801.
66 M. Lund, R. Vacha and P. Jungwirth, *Langmuir*, 2008, **24**, 3387–3391.
67 A. E. Garcia, H. Herce, and D. Paschek, *Simulations of Temperature and Pressure Unfolding of Peptides and Proteins with Replica Exchange Molecular Dynamics*, Elsevier, 2006, Volume 2.
68 T. Lazaridis and M. Karplus, *Proteins: Struct., Funct., Genet.*, 1999, **35**, 133–152.
69 R. Politi, L. Sapir and D. Harries, *J. Phys. Chem. A*, 2009, **113**, 7548–7555.
70 D. B. Knowles, A. S. Lacroix, N. F. Deines, I. Shkel and M. T. Record, *Proc. Natl. Acad. Sci. U. S. A.*, 2011, **108**, 12699–12704.
71 P. E. Mason, J. W. Brady, G. W. Neilson and C. E. Dempsey, *Biophys. J.*, 2007, **93**, L04–6.
72 S. Sukenik and D. Harries, *Prion*, 2012, **6**, 26–31.
73 P. A. Gurnev, D. Harries, V. A. Parsegian and S. M. Bezrukov, *J. Phys.: Condens. Matter*, 2010, **22**, 454110.